

Determination of $\text{Fe}^{2+}/\text{Fe}^{3+}$ mole ratio based on the change of precursor lattice parameters of wustite based iron catalysts for the ammonia synthesis

Artur Jurkowski, Zofia Lendzion-Bieluń*

West Pomeranian University of Technology, Faculty of Chemical Technology and Engineering, Institute of Inorganic Chemical Technology and Environment Engineering, Szczecin, ul. Piastów Ave. 42, 71-065 Szczecin, Poland

*Corresponding author: e-mail: Zofia.Lendzion-Bielun@zut.edu.pl

In the presented article, oxide forms of iron catalysts with the wustite structure and with a $R = \text{Fe}^{2+}/\text{Fe}^{3+}$ molar ratio in the range from 3.78 to 8.16 were investigated. The chemical composition of the tested catalyst precursors was determined by inductively coupled plasma optical emission spectrometry (ICP-OES). The X-ray diffraction (XRD) technique was used to determine the phase composition and location of reflections characteristic of the Fe_{1-x}O phase. The molar ratio of iron ions $R = \text{Fe}^{2+}/\text{Fe}^{3+}$ was determined by manganometric titration. The distribution of promoters in the structure of iron catalyst precursors with different $R = \text{Fe}^{2+}/\text{Fe}^{3+}$ ratio was determined by a selective etching method. The dependence of the lattice parameter a_o value in the crystal structure Fe_{1-x}O on the molar ratio $R = \text{Fe}^{2+}/\text{Fe}^{3+}$ was determined. On the basis of the determined dependence, R can easily be calculated in catalyst precursors of the wustite structure.

Keywords: wustite ammonia catalyst, XRD technique, manganometry, wustite lattice parameter.

INTRODUCTION

High activity in the synthesis reaction is demonstrated by a catalyst obtained from a precursor, which main component is iron(II) oxide Fe_{1-x}O called wustite¹. Wustite is a non-stoichiometric form of iron oxide of the formula Fe_{1-x}O , in which the Fe/O molar ratio is less than 1. The nonstoichiometric nature of this phase is related to building in of Fe^{3+} ions into the crystalline structure at the crystallization stage. The consequence of the higher content of Fe^{3+} ions with an ionic radius smaller than Fe^{2+} ions is the reduction of the interplanar spacings d and thus the value of the unit cell parameters.

In turn, the increase in the lattice parameter may also be caused by the incorporation of larger size ions into the network for example Ca^{2+} instead of Fe^{2+} ions. It is known from the current research results that the iron catalyst activity depends on the phase composition of the iron catalyst precursor and on the molar ratio of $\text{Fe}^{2+}/\text{Fe}^{3+}$ ions¹. Maximum activity is achieved by catalysts obtained as a result of the reduction of monophasic precursors, one crystallographic phase of Fe_{1-x}O with promoters evenly built-in into the structure, and a glass phase². Catalyst precursors in which the molar ratio of $\text{Fe}^{2+}/\text{Fe}^{3+}$ ions, denoted as R , is above 3.5 is considered to be monophasic. The activity of the iron catalyst in the ammonia synthesis reaction increases when R increases, until the maximum of the activity, for R equal to 5, is reached³. Further increase of R does not change the activity of the catalyst.

It was shown that the increase in the activity of the catalyst reduced from wustite along with the increase in R results from the higher exposure of the crystallographic planes (111) and (211) and the smaller proportion of less active planes (110) of iron in the form of a reduced catalyst⁴. The change in the phase composition of the precursor also influences the change in the ratio of the number of acidic to alkaline centers in the active form of the catalyst⁵. When R value increases in the iron catalyst precursors, the proportion of acid centers

increases too, what results in an increase in the activity in the ammonia synthesis reaction.

In addition, the increase in R value in the iron catalyst precursor lowers the reduction temperature of the wustite catalyst precursor compared to magnetite⁶. The effect of the reduction temperature lowering is a significant reduction in the energy consumption of the catalyst preparation process in industrial installations.

As can be seen, R in the wustite catalyst precursor has a significant effect on the structure and surface properties that are correlated with the activity of the active phase. Precursors of iron catalysts are produced by melting magnetite with promoters⁷. The R ratio in the wustite catalyst precursor and chemical composition are formed at the initial stage of production. The preparation of an appropriate batch mixture for the melting process is an important element in terms of chemical composition and the amount of reducer. The conditions of the crystallization process that influence the distribution of promoters in the catalyst precursor structure⁸ are also very important.

One of the methods for determining the molar ratio of $R = \text{Fe}^{2+}/\text{Fe}^{3+}$ ions in iron catalyst precursors is the manganometric titration method⁹. The main disadvantages of this method are time consumption and the necessity to use expensive, dangerous to health and environmental reagents such as HgCl_2 , SnCl_2 .

The paper investigates the change of wustite cell parameters (a_o) in a series of iron catalyst precursors with a wustite structure with different $\text{Fe}^{2+}/\text{Fe}^{3+}$ molar ratio denoted as R . The distribution of promoters in the structure of precursors differing by R was also examined.

The dependence of the lattice constant of Fe_{1-x}O phase for a series of wustite catalysts on the ratio of iron ions $R = \text{Fe}^{2+}/\text{Fe}^{3+}$, $a_o = f(R)$, has been presented.

EXPERIMENTAL

Precursors of wustite catalysts were obtained in a laboratory installation for the melting of catalysts – detailed

description can be found in the literature^{7, 10}. Magnetite, calcium oxide, aluminum oxide, potassium nitrate(V), and metallic iron as a reducer were used to prepare the catalyst precursors. Various ratios of reducer to magnetite allowed to obtain the precursors of catalysts with different R. After the reagents were completely melted, the lava was drained and cooled down to room temperature. The chemical composition of the obtained catalyst precursors was examined by inductively coupled plasma optical emission spectrometry (ICP-OES). The Optima 5300DV spectrometer from Perkin Elmer was used for the measurements. The solutions of the tested catalyst precursors were prepared by dissolving samples of 0.1 g in Merck hydrochloric acid at a concentration of 30%. The dissolution process was carried out at an elevated temperature using a Milestone microwave oven.

The solution was then quantitatively transferred to a 100 ml volumetric flask and refilled with deionized water.

Scanning electron microscope (SEM) UHR FE-SEM Hitachi SU8020 and attached energy-dispersive X-ray spectroscopy (EDS) system were used for the investigation of the morphology and composition of the wustite based catalyst surface.

The phase composition was determined by X-ray diffraction (XRD) with the Philips X'Pert Pro apparatus. The source of X radiation was a CoK_α lamp. The phase composition and positions of reflections 2θ were determined using the X'Pert HighScore Plus software.

The R ratio was determined by the managometric titration. This method consists in titration with potassium permanganate of the solution of the dissolved catalyst precursor. The leaching in hydrochloric acid solution is carried out in an inert atmosphere to prevent the oxidation of Fe^{2+} iron ions. In the first stage of the analysis, the number of moles of Fe^{2+} ions is determined. The second part involves the reduction of iron ions in the third oxidation state using tin(II) chloride to determine the total moles of iron in the sample.

Distribution of promoters in the structure of the oxidized form of the catalyst was examined by the selective etching method⁹. Catalyst precursors with different R were dissolved in solutions of hydrochloric acid of various concentrations and different contact times.

The ICP-OES method with Optima 5300DV PerkinElmer spectrometer was used to analyze the chemical composition of the solutions. Based on the results, the dependence of the degree of etching of the promoter oxides on the degree of iron dissolution was determined.

RESULTS AND DISCUSSION

The chemical composition and R of the tested catalyst precursors are presented in Table 1. The ratio of iron ions R changed in the investigated precursors in the range from 3.78 to 8.16. The contents of individual oxides were: Al_2O_3 in the range from 1.81 wt.% to 4.11 wt.%, CaO from 1.63 wt.% to 2.98 wt.%, and for K_2O from 0.39 wt.% to 0.82 wt.%.

The iron catalyst precursors are composed of iron oxide grains with built-in promoters and intergranular space Fig. 1. In the precursors of catalysts, grains are built of iron(II) oxide, Fe_{1-x}O , and structure promoters

Table 1. Chemical composition and R of the tested catalyst precursors

Lp.	R	Promoters concentration, [wt. %]		
		Al_2O_3	CaO	K_2O
1.	3.78	2.00	1.70	0.42
2.	3.93	1.96	1.65	0.43
3.	4.25	2.01	1.73	0.47
4.	4.96	2.13	1.63	0.39
5.	5.02	2.29	1.80	0.45
6.	5.34	2.25	2.04	0.49
7.	6.38	1.81	1.63	0.39
8.	7.36	3.74	2.46	0.71
9.	7.53	3.77	2.74	0.71
10.	7.72	4.11	2.93	0.82
11.	8.16	3.92	2.98	0.81

such as calcium oxide and aluminum¹¹. Grain spaces are filled with calcium and aluminum oxides, that are not build in into the catalyst grain, in the form of such compounds as, for example, CaAl_2O_4 , Al_2FeO_4 , CaSiO_3 and potassium oxide in the form of K_2O , K_2SiO_3 ¹².

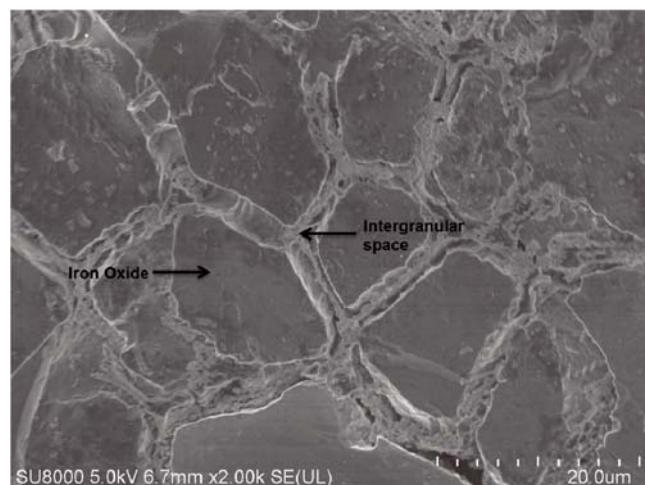


Figure 1. SEM image of the oxidized form of wustite based catalyst

The X-ray patterns of catalyst precursors with different R are shown in Figure 2. The reflections at positions 2θ 36°, 41.8°, 60.7°, 72.7°, and 75.5° visible on diffraction patterns correspond respectively to planes (111), (200), (220), (311), (222) in the crystalline structure of the wustite phase based on the [ICDD 99-001-0002] card. The analysis of the spectra obtained allowed to state that the tested catalyst precursors are monophasic systems.

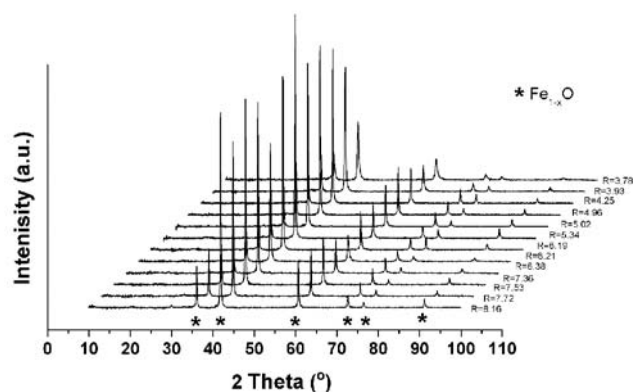


Figure 2. X-ray patterns of the catalyst precursors with different R

Comparing the positions of the maxima of reflections for individual crystallographic planes in different catalyst precursors, it can be seen that the reflections are not at the same angles. Reflections for the plane (200) are shown in Fig. 3. As the R increases, the reflex moves toward the lower angles.

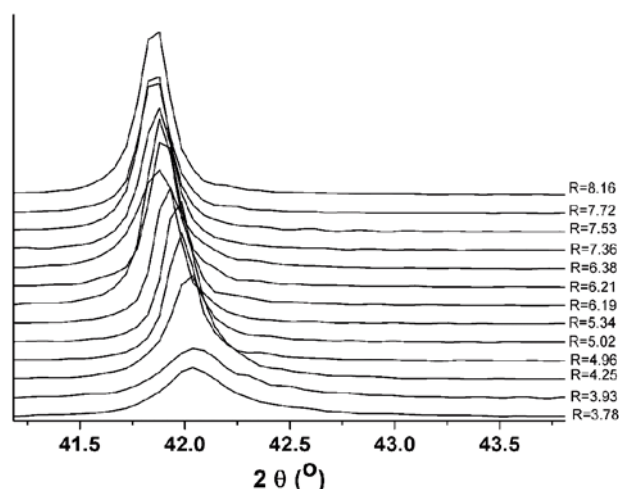


Figure 3. The shift of the reflex maxima for the plane (200) in the catalyst precursors with different R

On the basis of the obtained diffraction patterns, the values of lattice constants a were determined for the tested catalyst precursors. The lattice constant a_0 for each catalyst precursor was determined by plotting the linear dependence of parameter a , determined for each Θ , in the function of $(\cos^2\Theta / \sin \Theta + \cos^2 \Theta / \Theta)$. Parameter a_0 is the value of the function at the point of its intersection with abscissa axis. Figure 4 shows the dependence of the a_0 change in the function of x . The value x was determined from equation 1 describing the dependence of x in Fe_{1-x}O and the molar ratio R:

$$x = 1 / (3 + 2 \cdot R) \quad (1)$$

the Fig. 4 additionally contains literature data in which a linear relationship between the Fe/O ratio and the lattice constant (a_0) has been confirmed^{6, 13}.

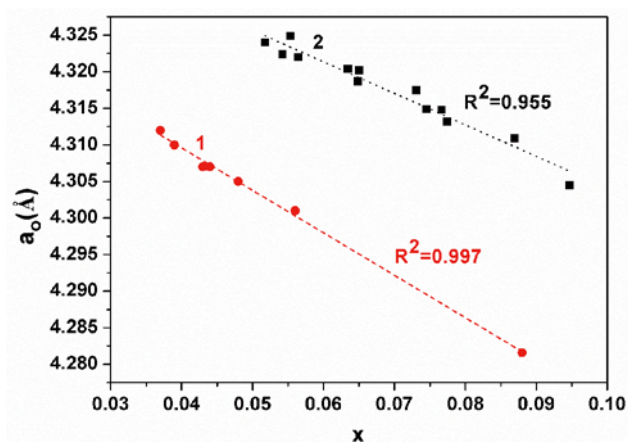


Figure 4. Relationships between wustite cell dimension and x in Fe_{1-x}O . (1) – literature data [12], (2) – data for the investigated catalyst precursors

The dependence presented for the literature data (1) is based on tests carried out for pure wustite. The observed changes of the lattice constant in the wustite were related to the change in the oxygen content in

the wustite elementary cell obtained under different temperature conditions. Curve 2 shows the change in the lattice constant and in iron oxide precursors in which promoter ions such as calcium and aluminum are incorporated into the wustite cell structure. Both the preparation conditions and the presence of additional ions in the wustite structure affect the value of the network constant, which may explain the apparent shift between curves 1 and 2 in the figure.

In order to investigate the influence of R on the degree of incorporation of aluminum, calcium, and potassium oxide into the grain of the oxidized form of the wustite catalyst, the distribution of promoters in precursor structures with different R was examined by the selective etching method. The catalyst precursors with $R = 6.38$ and $R = 4.25$ were selected for comparison. The precursor oxide forms have been selected due to similar chemical composition and the largest possible difference in R. Fig. 5 shows the results of selective etching catalyst of $R = 6.38$. By plotting the dependence of the degree of iron dissolution on the degree of dissolution of individual promoters, a characteristic inflection can be noticed. This point corresponds to the percentage of promoters in the intergranular space in relation to the total content of oxides in the catalyst precursor. About 57% weight of total Al_2O_3 and approx. 38% weight of total CaO is located in the intergranular space. The remaining amounts of alumina and calcium dissolve evenly with the digestion of the iron oxide forming the catalyst grain. Potassium oxide in 99% by mass was located in intergranular spaces.

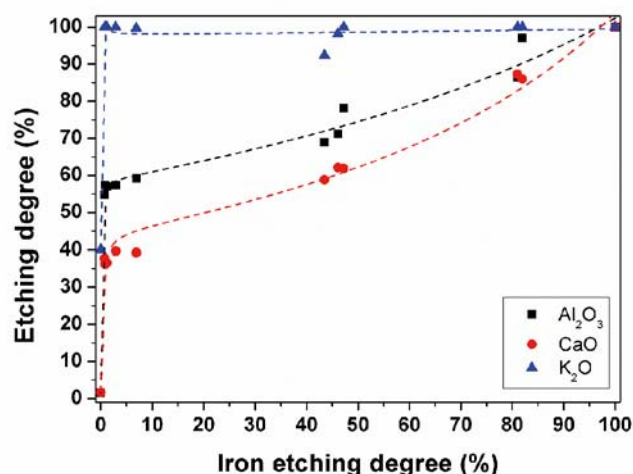


Figure 5. Etching curve for the catalysts with $R = 6.38$

In the case of the $R = 4.25$ catalyst, Fig. 6, the curve inflexion for Al_2O_3 corresponds to 58% by mass, whereas calcium, as in the case of the precursor with $R = 6.38$, is 38%. The solubility of Ca^{2+} ions in the wustite is higher than in other iron oxides⁹. Calcium ions, due to similar valence shell to Fe^{2+} ions are easier to integrate into the wustite crystal lattice, entering into the vacancy defect or substituting Fe^{2+} ions. On the other hand, Al^{3+} ions, due to the same valence shell structure as Fe^{3+} , integrate seamlessly into the structure of Fe_3O_4 to form a solid solution of FeAl_2O_4 with the same crystallographic structure as Fe_3O_4 ¹³. In the wustite Al_2O_3 , a substitutional solid solution that builds up to a lesser

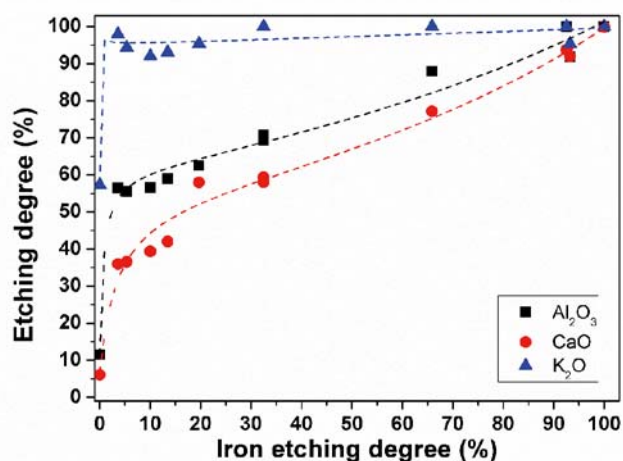


Figure 6. Dependence of etching degree of promoters calcium, potassium and aluminium oxide, on the degree of iron in the catalyst precursor with $R = 4.25$

extent due to the larger obstacles caused by varying degrees of oxidation.

Based on the data from the etching curves and chemical composition, concentrations of calcium and aluminum oxides in the intergranular spaces and grains of the tested catalyst precursors were calculated. Calculated results are shown in Table 2. Additionally, the table presents data for the catalyst with $R = 5.34$, for which promoter distribution studies were also carried out.

Table 2. Concentration of aluminum and calcium oxides in catalyst grain and intergranular space

Lp.	R	Concentration in intergranular space [%]		Concentration in catalyst grain [%]	
		Al ₂ O ₃	CaO	Al ₂ O ₃	CaO
1	6.38	1.03	0.62	0.78	1.01
3	5.34	1.42	1.10	0.83	0.94
2	4.25	1.12	0.66	0.88	1.07

The change of R does not cause a significant change in the degree of incorporation of individual promoters into the grains of these catalysts. It can be noticed that with the increase of R the aluminum concentration in the wustite grain decreases slightly. Concentration of calcium oxide in the wustite grains is on the constant level. Based on the results, it can be assumed that the use of similar amounts of promoters in the catalyst precursors will not affect the value of the lattice constant and the wustite phase.

Figure 7 shows the dependence of the network constant a_o in the R function.

With the increase of R , the defect of the wustite lattice by Fe^{3+} ions decreases. The oxygen concentration in the wustite cell increases, which in turn leads to an increase in the lattice constant a_o . The equation describing the dependence $R = f(a_o)$ was determined:

$$y = 9145.1981 \cdot x^2 - 78706.6649 \cdot x + 169347.8715 \quad (2)$$

Using the equation based on the determined lattice constant, one can determine the molar ratio of iron ions Fe^{2+} / Fe^{3+} for tested iron catalyst precursors with a wustite structure.

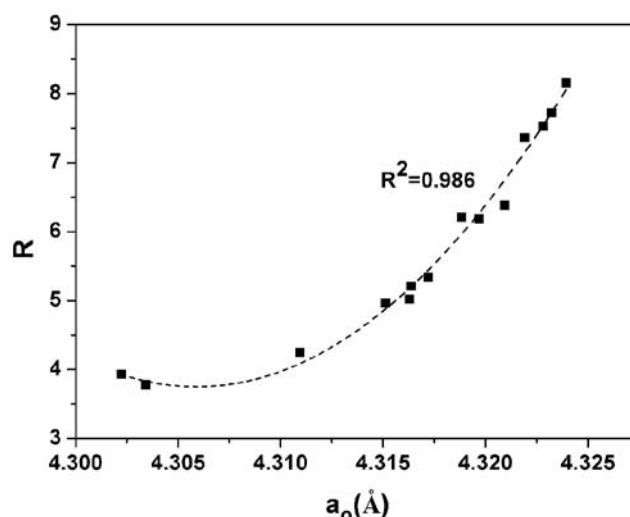


Figure 7. Change in unit cell dimension of the precursor catalysts based wustite

CONCLUSIONS

In the work, wustite based catalyst precursors with different R iron ions ratio and similar chemical composition of the promoters were used. A change in the molar ratio of Fe^{2+} to Fe^{3+} ions in the precursor results in a shift of the maximum reflections on the X-ray diffraction pattern of the wustite phase. That shift is related to the change of the cell constant of the wustite elementary cell. It has been shown that based on the determined value of the network constant, it is possible to determine the ratio of iron ions on the second and third oxidation states in the iron oxide catalyst precursor with a wustite structure. This method can be used instead of the traditional method of manganometric titration to determine the ratio of $R = Fe^{2+}/Fe^{3+}$ ions. This is particularly important at the stage of controlling during the wustite catalyst production process.

ACKNOWLEDGMENT

This work was supported by the Polish National Research and Development Centre No. Tango2/340001/NCBR/2017

LITERATURE CITED

1. Liu, H.Z., Li, X.N. & Hu, Z.N. (1996). Development of novel low temperature and low pressure ammonia synthesis catalyst. *Appl. Catal. A Gen.* 142(2), 209–222. DOI: 10.1016/0926-860X(96)00047-6.
2. Liu, H. & Li, X. (1997). Relationship between Precursor Phase Composition and Performance of Catalyst for Ammonia Synthesis. *Ind. Eng. Chem. Res.* 36(2), 335–341. DOI: 10.1021/ie960072s.
3. Liu, H. (1986). China Patent no. 86108528.0.
4. Zheng, Y.F., Liu, H.Z., Liu, Z.J. & Li, X.N. (2009). In situ X-ray diffraction study of reduction processes of Fe_3O_4 - and $Fe_{1-x}O$ -based ammonia-synthesis catalysts. *J. Solid State Chem.* 182(9), 2385–2391. DOI: 10.1016/j.jssc.2009.06.030.
5. Liu, H. & Han, W. (2017). Wüstite-based catalyst for ammonia synthesis: Structure, property and performance. *Catal. Today*, 297, 276–291. DOI: 10.1016/j.cattod.2017.04.062.
6. Pernicone, N., Ferrero, F., Rossetti, I., Forni, L., Canton, P., Riello, P., Fagherazzi, G., Signoretto, M. & Pinna, F. (2003).

Wustite as a new precursor of industrial ammonia synthesis catalysts. *Appl. Catal. A Gen.* vol. 251(1). 121–129. DOI: 10.1016/S0926-860X(03)00313-2.

7. Jedrzejewski, R. & Lendzion-Bieluń, Z. (2018). Reduction Process of Iron Catalyst precursors for Ammonia Synthesis Doped with Lithium Oxide. *Catalysts*. 8(11). 494. DOI: 10.3390/catal8110494.

8. Lendzion-Bieluń, Z., Jędrzejewski, R., Ekiert, E. & Arabczyk, W. (2011). Heterogeneity of ingot of the fused iron catalyst for ammonia synthesis. *Appl. Catal. A Gen.* 400. 48–53. DOI: 10.1016/j.apcata.2011.04.010.

9. Lendzion-Bieluń, Z. & Arabczyk, W. 2001. Method for determination of the chemical composition of phases of the iron catalyst precursor for ammonia synthesis. *Appl. Catal. A Gen.* 207(1-2). 37–41. DOI: 10.1016/S0926-860X(00)00614-1.

10. Arabczyk, M.J.W., Ziebro, J., Kałucki, K. & Świerkowski, R. (1996). Instalacja do ciągłego wytopu katalizatorów żelazowych. *Chemik*. 1. 22–24.

11. Lendzion-Bieluń, Z., Arabczyk, W. & Figurski, M. The effect of the iron oxidation degree on distribution of promoters in the fused catalyst precursors and their activity in the ammonia synthesis reaction. *Appl. Catal. A Gen.* vol. 227(1-2). 255–263. DOI: 10.1016/S0926-860X(01)00938-3.

12. Han, W., Huang, S., Cheng, T., Tang, H., Li, Y. & Liu, H. (2015). Promotion of Nb₂O₅ on the wustite-based iron catalyst for ammonia synthesis. *Appl. Surf. Sci.* 353. 17–23. DOI: 10.1016/j.apsusc.2015.06.049.

13. Chaklader, A.C.D. & Blair, G.R. (1970) Differential thermal study of FeO and Fe₃O₄. *J. Therm. Anal.* 2(2). 165–179. DOI: 10.1007/BF01911348.

14. Figurski, M.J., Arabczyk, W., Lendzion-Bieluń, Z., Kałęczuk, R.J. & Lenart, S.X. On the distribution of aluminium and magnesium oxides in wustite catalysts for ammonia synthesis. *Appl. Catal. A Gen.* 247(1). 9–15. DOI: 10.1016/S0926-860X(03)00084-X.